

Minimization of suboxide transition regions at Si–SiO₂ interfaces by 900 °C rapid thermal annealing

G. Lucovsky,^{a)} A. Banerjee, B. Hinds, B. Clafin, K. Koh, and H. Yang
*Departments of Physics, Materials Science and Engineering, Electrical and Computer Engineering,
and Chemistry, North Carolina State University, Raleigh, North Carolina 27695-8202*

(Received 17 February 1997; accepted 10 April 1997)

Transitions regions at Si–SiO₂ interfaces contain excess suboxide bonding arrangements which contribute to interface roughness and also can give rise to electronically active defects. This article provides insights into the origin and temperature stability of these suboxide bonding arrangements by studying different interface formation processes, e.g., rapid thermal oxidation and plasma-assisted oxidation, and then subjecting these interfaces to rapid thermal annealing (RTA). The interfacial bonding chemistry has been studied before and after the RTA by Auger electron spectroscopy and it has been demonstrated that interfacial transition regions with suboxide bonding are a direct result of thermal and plasma-assisted oxidation at temperatures up to at least 800 °C, and that the excess suboxide bonding in interfacial transition regions is significantly reduced following a 30 s, 900 °C RTA. The kinetics of this interfacial annealing process are essentially the same as observed for the RTA-induced separation of homogeneous suboxide thin films (SiO_x, x < 2) into silicon nanocrystals and stoichiometric SiO₂. © 1997 American Vacuum Society.
[S0734-211X(97)07004-2]

I. INTRODUCTION

As channel lengths of field effect transistors (FETs) decrease into the deep submicron to 0.1–0.05 μm to provide increased levels of device integration, there must be accompanying decreases in gate oxide thicknesses (t_{ox}) initially to 3 nm and ultimately to <2 nm in order to maintain the drive currents needed for circuit operation. Once gate oxide thicknesses are reduced to a regime where direct tunneling occurs, e.g., <3 nm, the planarity of the gate oxide interfaces with both the channel region and gate electrode of the FET structure becomes a crucial issue since atomic scale variations in the effective gate oxide thickness can lead to order of magnitude variations in local tunneling currents. This article focuses on excess suboxide bonding arrangements that contribute to atomic scale roughness at Si–SiO₂ interfaces. It is important to recognize that interface roughness at the SiO₂-gate electrode interface must also be addressed since variations in the tunneling thickness can be induced by the roughness at both interfaces of an ultrathin gate oxide.

At an ideal Si(111)–SiO₂ interface with single Si dangling bond termination, the bonding arrangements can be characterized as Si–Si₄ in the Si substrate (the subscript indicates the number of Si atoms bonded to the reference Si atom), Si–O₄ in the bulk of the oxide, and Si–Si₃O at the metallurgical boundary. The Si–Si₃O bonding arrangement is one of three suboxide bonding arrangements; the other two are Si–Si₂O₂ and Si–SiO₃. If the interface between the Si substrate and the SiO₂ is not perfectly flat, then there must be additional or excess suboxide bonding arrangements that define a *transition region* between the Si substrate and a stoichiometric *bulk* oxide. This means that there is inherently a direct relationship between *excess* suboxide bonding ar-

rangements, interfacial transition regions, and interfacial roughness. Assuming that the top surface of the oxide is perfectly flat, localized tunneling (either direct or Fowler–Nordheim) above an average value will take place at those interface locations where these excess suboxide bonding arrangements *extend into* the oxide and reduce the thickness through which electrons tunnel.

The issue of interfacial roughness and transition regions with excess suboxide bonding is further complicated by experimental observations that interfacial nitridation improves device reliability, at least in N-channel devices.^{1,2} This means that interface roughness may involve both Si–O and Si–N bonding arrangements in the nitrated structures. This article addresses roughness and suboxide bonding at Si–SiO₂ interfaces prepared by (i) remote plasma-assisted oxidation (RPAO) using O₂ and N₂O source gases,³ and (ii) rapid thermal oxidation (RTO) in O₂ and N₂O, and compares results of these studies with thermal oxidation in O₂.

Section II presents new experimental data obtained by on-line Auger electron spectroscopy (AES) that demonstrates changes in bonding at Si–SiO₂ interfaces after interfaces formed by RPAO and RTO at temperatures of 300 and 800 °C, respectively, and subjected to 30 s RTAs at 900 °C. The aspect of the present work that distinguishes it from past studies is the systematic control or processing conditions, in particular the separate and independent control of interface formation by RPAO and RTO at temperatures ≤800 °C and interface relaxation by RTA at 900 °C. Section III compares the results of this study with recent results of other studies that have addressed the thermal stability of bulk homogeneous suboxides,^{4,5} as well as x-ray photoelectron spectroscopy (XPS) studies that have directly addressed chemical bonding in the interfacial transition regions.^{6–8} Interfacial roughness and suboxide transition regions have also been

^{a)}Electronic mail: gerry.lucovsky@ncsu.edu

studied by x-ray scattering,⁹ medium energy ion scattering (MEIS),¹⁰ and transmission electron microscopy (TEM) imaging.¹¹ This paper also includes experimental results from second-harmonic generation (SHG) studies that bear on the issue of suboxide bonding (see Ref. 3 and Refs. therein).

II. EXPERIMENTAL RESULTS

The new AES results presented in this article have been obtained using an ultrahigh vacuum (UHV) compatible multichamber system that has separate chambers for remote plasma processing (RPP), rapid thermal processing (RTP), and on-line AES. This system provides for (i) fabrication of Si–SiO₂ interface structures by either RPAO or RTO, and then (ii) structural and chemical relaxation of these interfaces by RTA. Two different oxygen/nitrogen atom source gases have been used: O₂ and N₂O.³ For both the RPAO and RTO processes, the surfaces of high resistivity $\sim 10 \Omega \text{ cm}$ p-type Si wafers were prepared by a two-stage process: high temperature ($\sim 900 \text{ }^\circ\text{C}$) thermal oxidation to grow a sacrificial oxide layer that is subsequently removed by rinsing in dilute HF. Wafers were then inserted into the plasma processing chamber of the system via a load lock sample introduction chamber. For the RPAO process, they were heated to $300 \text{ }^\circ\text{C}$ at the chamber base pressure, $\sim 10^{-8}$ Torr, and then subjected to plasma-assisted oxidation. The RPAO process has been previously used as the first step of a two step process for the formation of gate oxides.¹² In addition to forming a superficially thin oxide, $\sim 0.5 \text{ nm}$, the RPAO process reduces levels of interface contamination, e.g., residual C and F concentrations are at the 10^{12} cm^{-2} range.² In the application of RPAO to gate oxide fabrication, $\sim 0.5\text{--}6 \text{ nm}$ of oxide is grown at $300 \text{ }^\circ\text{C}$ by remote plasma excitation of either He/O₂ or He/N₂O mixtures (rf power of $\sim 30 \text{ W}$ at 13.56 MHz) and this is followed by remote plasma enhanced chemical deposition (RPECVD) of the remainder of the oxide film.^{2,12} Thicker films with t_{ox} to $\sim 1.5 \text{ nm}$, have also been grown directly by the RPAO process by extending the oxidation time.³ The oxidation process kinetics have been characterized by a power law relation; e.g., for growth in O₂, $t_{\text{ox}} \sim 0.7t^{0.28}$, where t is the time in minutes. The power law representation means that the oxidation is very fast initially when plasma-generated excited O species interact with Si atoms that are not bonded to other O atoms, but then the oxidation rate slows down significantly when the oxidation involves Si atoms that are bonded to O as well as other Si atoms. The RTO process was performed at $800 \text{ }^\circ\text{C}$ with a source gas flow rate of $2,000 \text{ sccm}$.

Figures 1(a) and 1(b) indicate oxide growth in using remote plasma excited mixtures of He/O₂ or He/N₂O, respectively, as monitored by on line AES. The oxide thickness is determined from the ratio of the relative amplitudes of the Si–Si AES feature at $\sim 92 \text{ eV}$ and the Si–O feature at $\sim 76 \text{ eV}$.¹² Films prepared using the He/N₂O source gas show nitrogen atom incorporation localized in the immediate vicinity of the Si–SiO₂ interface, as evidenced by a N_{KLL} AES feature and confirmed by secondary ion mass spectrometry (SIMS) and optical SHG.^{2,3} There is an AES spectral

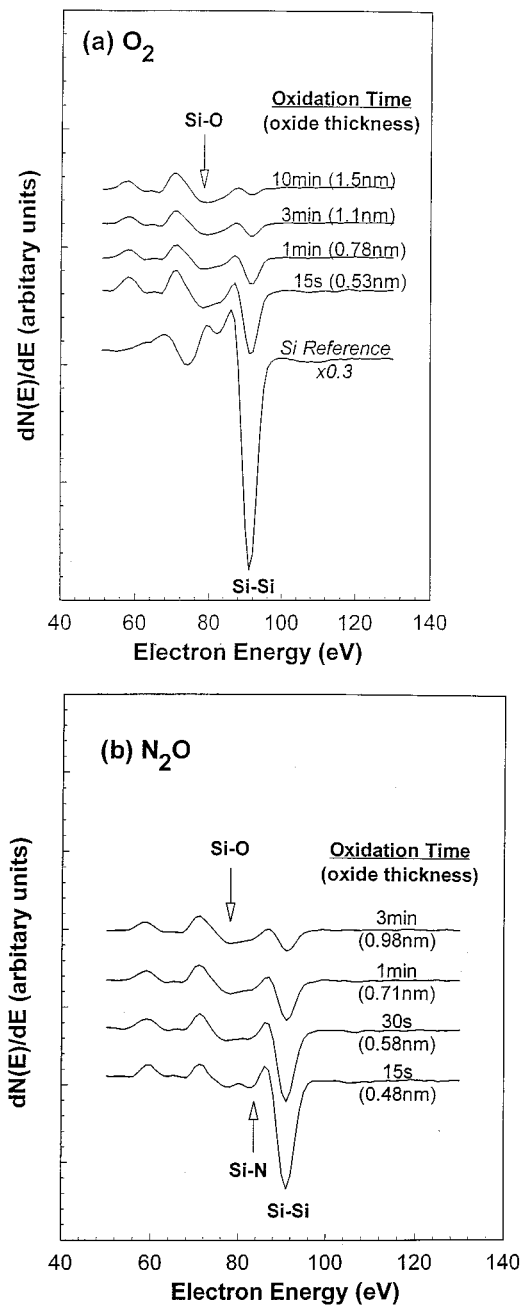


FIG. 1. Oxide growth in using remote plasma excited mixtures of (a) He/O₂ or (b) He/N₂O, respectively, as monitored by on line AES.

feature at $\sim 83 \text{ eV}$ in the Si_LVV region that has a contribution from Si–N bonding as well as an additional contribution from suboxide bonding arrangements. The contribution from suboxide bonding is identified by studies of the initial stages of oxidation before monolayer coverage has been obtained, whereas the contribution from Si–N has been verified by studying the interface between Si₃N₄ and Si. It is difficult to quantify the contribution to derivative AES spectra for the case in which both Si–N and suboxide bonding are present at the same time. However, as we show later on in the article, the relative changes in the derivative AES spectra after RTA are self-consistent, and are in agreement with the results of

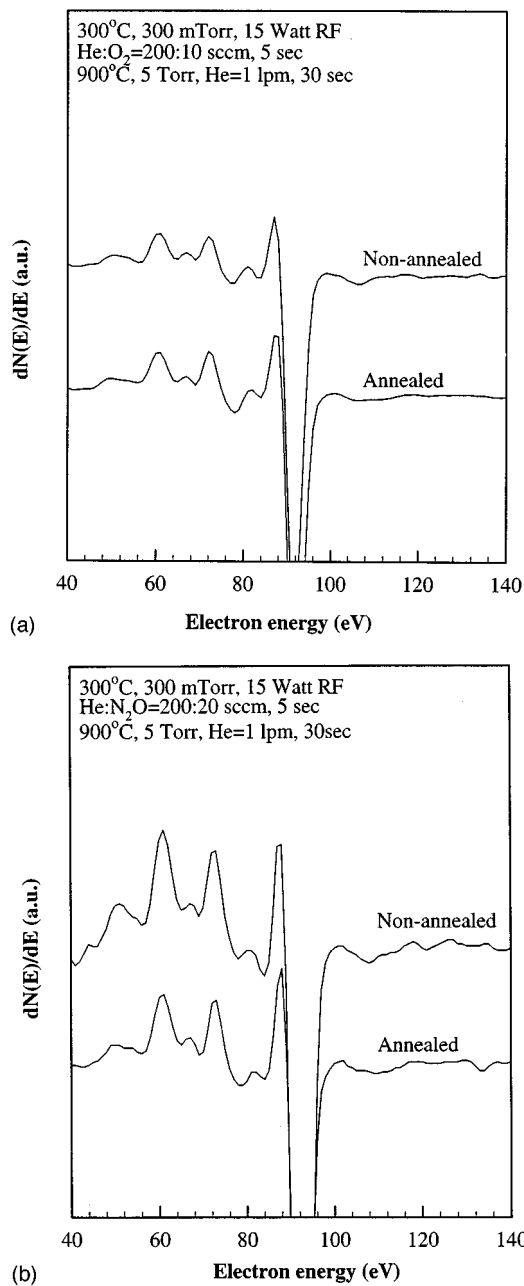


FIG. 2. Derivative Si_{L_{VV}} AES spectra for oxide layers grown in (a) He/O₂ and (b) in He/N₂O, respectively, by RPAO that are ~0.5 nm thick as grown at 300 °C and after a 30 s 900 °C RTA.

other experimental probes of interface roughness before and after a 900 °C RTA or equivalent thermal exposure.

Figures 2(a) and 2(b) indicate derivative Si_{L_{VV}} AES spectra for oxide layers prepared by RPAO using (a) He/O₂ and (b) in He/N₂O, respectively. These layers are ~0.5 nm thick as grown at 300 °C and after a 30 s 900 °C RTA. From the traces shown in Fig. 2 and the results in Table I, it is observed that the relative amplitude ratio, $[I(83 \text{ eV})/I(76 \text{ eV})]_{\text{after RTA}} / [I(83 \text{ eV})/I(76 \text{ eV})]_{\text{before RTA}}$, decreases after the anneal. Figures 3 and 3(b) indicate similar spectra for films prepared by RTO in O₂ and N₂O at 800 °C, and after a 30 s 900 °C RTA. Smaller decreases in the am-

TABLE I. Changes in the relative intensities of the SiO_x and SiO₂ AES at ~83 eV and 76 eV, respectively.

Interface formation	$[I(83 \text{ eV})/I(76 \text{ eV})]_{\text{after RTA}} / [I(83 \text{ eV})/I(76 \text{ eV})]_{\text{before RTA}}$
Plasma O ₂	0.88 ± 0.02
Plasma N ₂ O	0.79 ± 0.02
RTO O ₂	0.80 ± 0.02
RTO N ₂ O	0.86 ± 0.02

plitude ratio occur for these samples. To confirm that changes in the amplitude ratio were not due to oxidation during the RTA, the relative amplitudes of the Si-Si Si_{L_{VV}} feature at ~92 eV, and the O_{KLL} feature at ~510 eV were also monitored and found to be the same before and after the RTA. Table I contains normalized amplitude ratios, $[I(83 \text{ eV})/I(76 \text{ eV})]_{\text{after RTA}} / [I(83 \text{ eV})/I(76 \text{ eV})]_{\text{before RTA}}$, for the results presented in Figs. 2(a), 2(b), 3(a), and 3(b). Since these ratios are all less than one, this means that there is a relative decrease in the amplitude of the 83 eV feature after the anneal.

III. DISCUSSION

Consider first the spectra in Figs. 2(a) and 2(b) for the as grown films. The feature at 76 eV is associated with Si-O bonding, in particular Si atoms with four oxygen atom neighbors. The AES results indicate that the feature at 83 eV has two contributions: (i) from Si-N bonds and (ii) from suboxide bonding arrangements, where the Si atom has one, two or three O atom neighbors. For example, AES results for films that display a relatively weak O_{KLL} feature, as in Fig. 2(a), also display a suboxide bonding feature at ~83 eV. In a more direct way, Tao *et al.*⁶ have shown significant reductions in suboxide bonding arrangements for films prepared by thermal oxidation at 600 °C, and then annealed at 925 °C consistent with changes in the AES features in films prepared by RTO and RPAO before and after 900 °C annealing. In particular, the concentration of suboxide bonding arrangements as determined from analysis of XPS data is reduced from ~3 monolayers by more than a factor of 2 after a 925 °C anneal. These changes in XPS are consistent with the AES intensity changes presented in Table I.

The effect of the 900 °C anneal in reducing suboxide bonding also helps to explain previously reported results from optical SHG measurements on oxidized vicinal Si(111) wafers off-cut in the 112 bar direction (Ref. 3 references therein). For the geometry of the measurements discussed in Ref. 3, the SHG signal comes predominantly from the Si-SiO₂ interface. These results are included in Table II which presents the results of experiments in which the azimuthal asymmetry has been addressed. The exciting source for these measurements is a Nd:YLF laser at 1.17 eV, and the Si(111) off-cut angles are approximately 5°. Experiments performed on thermally grown oxides subjected to rapid thermal annealing at 900 °C indicated a significant change in the rela-

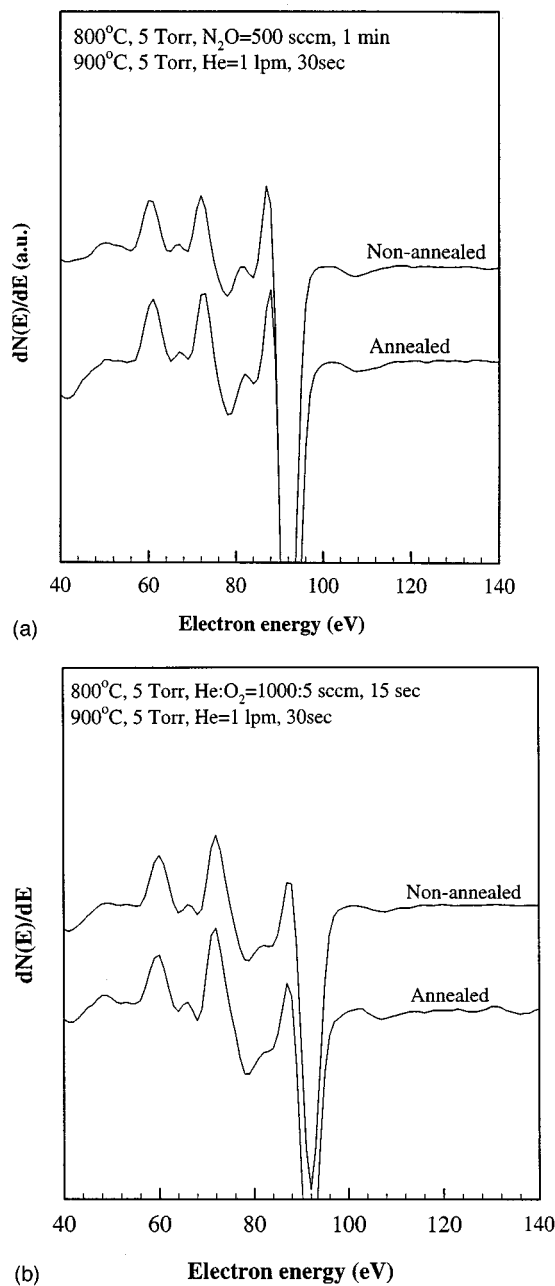


FIG. 3. Derivative Si_{L_{VV}} AES spectra for oxide layers grown in (a) He/O₂ and (b) in He/N₂O, respectively, by RTO that are ~0.5 nm thick as grown at 300 °C and after a 30 s 900 °C RTA.

tive phase of the SHG signals associated with the steps and terrace regions.¹³ The SHG signal for the vicinal wafers is given by

$$E(2\omega) = (A_1 \cos \Phi + A_3 \cos 3\Phi) [\exp(-i\Delta_{13})], \quad (1)$$

where A_1 and A_3 are the amplitudes of the harmonic signal components at Φ and 3Φ , Φ is the angle between the 112 direction and the incident electric field, and Δ_{13} is the relative phase. The relative phase is related to the difference in resonance energies between the two harmonic components of the second harmonic signal. From Table II, the relative phase of the as-grown thermal oxide is 72°, and decreases signifi-

cantly to ~23° after the 900 °C anneal.¹³ In a similar way the relative phases for interfaces formed by 300 °C RPAO also change markedly after a similar 30 s 900 °C RTA. There are no significant differences between Δ_{13} for RPAO interfaces formed in N₂O and O₂, even though SIMS and on-line AES show a nitrogen terminated interface for the N₂O process. However, after the RTA, there are significant differences in Δ_{13} . Δ_{13} is equal to 23° for the oxygen terminated interfaces, the same value as obtained after annealing a thermally grown interface, but is reduced to 11° for the nitrogen terminated interface. The SHG results are then consistent with a significant change in interface bonding. Combining the SHG results with the XPS and AES results we conclude that the Δ_{13} values of 67°–72° are then characteristic of suboxide bonding arrangements, whereas the smaller values of Δ_{13} of 23° and 11° are indicative, respectively, of more nearly idealized interface bonding arrangements.

We have also studied the stability of suboxide films prepared by RPECVD at low temperatures (250–300 °C) and then subjected to RTA.^{4,5} The as-deposited films are hydrogenated suboxides. The local order in these films has been studied by infrared (IR) by analyzing the spectroscopic changes in the Si–H bond-stretching mode as a function of the oxygen concentration, x , as in SiO _{x} , $0 \leq x < 2$.^{14,15} This analysis indicated that the as-deposited films were random chemically-ordered alloys with statistically determined bonding of Si and O atoms in Si–Si₄, Si–Si₃O, Si–Si₂O₂, Si–SiO₃, and Si–O₄ local arrangements. Films for the annealing studies were prepared by RPECVD and then subjected to 30 s RTAs at 900 °C.^{4,5} Characterization of these films by IR indicated significant changes in the local bonding. Prior to the anneal, the films displayed a Si–O bond-stretching mode frequency between ~1010 and 1040 cm⁻¹ characteristic of homogeneous SiO _{x} alloys,^{14,15} and after the anneal the films displayed an Si–O bond-stretching mode frequency of ~1075 cm⁻¹, characteristic of stoichiometric SiO₂. Studies of the same films by TEM showed a homogeneous, noncrystalline character as-deposited, and a separation into Si nanocrystals (typical dimensions ~10 nm) embedded in a homogeneous amorphous matrix which was identified by IR as SiO₂.

The as-deposited homogeneous films showed strong photoluminescence at 80 K in a broad band extending from about 1.4 to 2.0 eV with the peak photon energy increasing as the x increased. This type of luminescence has been previously reported for homogeneous suboxide films.^{16,17} The annealed films displayed no detectable photoluminescence in the same spectral range. The absence of this type of luminescence in the annealed films is consistent with there being no significant suboxide regions at the interfaces between the Si nanocrystals and the encapsulating oxide films. Nanocrystals exposed to atmospheric oxygen and water vapor display characteristic suboxide bonding.¹⁸

Finally, recent studies of the kinetics of the process by which bulk suboxides, SiO _{x} , convert to Si nanocrystals encapsulated in SiO₂ or SiO _{x'} ($x > x'$) has been studied.⁵ These studies have demonstrated that the separation process is lim-

TABLE II. Summary of results from studies of vicinal Si(111) surfaces off-cut $\sim 5^\circ$ in the 112 bar direction.

Surface treatment ^a	Phase, $\Delta\Phi^b$	A_1/A_3^c
Plasma processing		
O ₂ - 15 s - 300 °C	68	0.20±0.02
O ₂ - 15 s - 30 s 900 °C RTA (0.5O ₂ /Ar)*	23	0.35±0.03
N ₂ O - 15 s - 300 °C	67	0.21±0.02
N ₂ O - 15 s - 30 s 900 °C RTA (Ar)	11	0.37±0.04
N ₂ O - 30 s - 300 °C	65	0.17±0.02
N ₂ O - 30 s - 30 s 900 °C RTA (Ar)*	11	0.35±0.03
Thermally grown interfaces		
Furnace oxidation at 850 °C	72	0.19±0.02
Post-oxidation anneal [30 s at 950 °C (0.5% O ₂ /Ar)]	23	0.33±0.03

^aPre-deposition RPAO step.

^bSee Eq. (1).

^cProcessing conditions for optimum electrical properties (see Ref. 2).

ited by reaction kinetics, and that the time constants for the bulk separation at temperatures of the order of 900 °C are essentially the same as those for the interface relaxation process, e.g., complete separation takes place in ~ 30 at 900 °C.

There are three other recently reported studies that have addressed surface roughness/interfacial transition regions and changes that take place on annealing. Gibson *et al.* have used TEM interference techniques and demonstrated significant interfacial smoothing for thermally grown oxides subjected to a 900 °C anneal.¹¹ Downer and co-workers have used optical SHG to study Si–SiO₂ interfaces formed on Si(100) and have observed irreversible changes in the response from interfaces formed at low temperatures, ~ 800 °C, that were subsequently subjected to 900 °C thermal exposure.¹⁹ Finally, Matsumura and co-workers showed that ultrathin oxides (~ 3 nm thick) prepared by thermal oxidation at 650 °C and annealed at 850 °C showed improved performance with respect to stress-induced increases in tunneling currents.²⁰ They also found that oxides grown at 850 °C showed improved stress resistance after an anneal at 850 °C. These improvements were correlated with reductions in interface roughness as measured by x-ray scattering techniques.

IV. SUMMARY

The results presented in this article have demonstrated that for interfaces formed by conventional thermal oxidation, RTO and RPAO at temperatures below 800 °C show significantly reduced suboxide bonding after a relatively short RTA at 900 °C. Reductions in suboxide bonding, or equivalently increased interface smoothness, have been observed by a variety of different experimental techniques including (i) AES, (ii) XPS,^{6,7} (iii) optical SHG,³ (iv) x-ray scattering,⁹ and TEM.¹ Comparisons between the annealing of homogeneous bulk suboxide films, which results in the formation of Si nanocrystals encapsulated in SiO₂, and the interface relaxation process, suggest that both processes are limited by similar reaction kinetics.

The results presented in this article, combined with the results of other studies cited above indicate that the formation of suboxide bonding is inherent in the oxidation of crys-

talline Si independent of the oxidation process for oxidation processes that are performed at temperatures up to at least 900 °C. This has previously been reported for thermal oxidation, and the results in this article extend this observation to other oxidation mechanisms.^{21,22} If this is indeed the case, then the chemical and structural relaxations that take place during the 900 °C RTAs, or equivalent thermal exposures, will determine the limiting values of interface smoothness attainable. For example, suppose that oxidation takes place on an atomically smooth surface and that this process results in some degree of suboxide bonding. After the oxidation process is concluded there will be some degree of suboxide bonding/interface roughness. Following a 900 °C anneal, there will be interface smoothing accompanied by a reduction of suboxide bonding arrangements. However, since the roughening that takes place during oxidation, and the smoothing that takes place during the anneal are causing changes in atomic scale structure, it is more than likely that *complete* smoothing will not take place; i.e., that there will always be some degree of suboxide bonding above and beyond what is ideal for the particular crystallographic orientation of the Si substrate, independent of the initial state of the Si surface prior to oxidation. This explains an experimental observation that interfaces formed on smooth Si surfaces in different ways, e.g., by thermal oxidation, RTO, and RPAO, and then subjected to thermal exposures at 900–1000 °C after interface formation, show essentially the same degrees of interface roughness as monitored by the field dependence of the channel mobility in FETs.²³ Finally, the residual surface roughness and associated suboxide bonding arrangements may also be the origin of the limiting values of midgap interface defect states (D_{it}) of about 10^{10} cm⁻² eV⁻¹. The lack of distinct spectral feature in this midgap region suggests that the states contributing to D_{it} are not silicon atom dangling bond states. This has been confirmed by the recent experiments of Stathis and co-workers at IBM.²⁴ We suggest that the midgap D_{it} may be derived from changes in local dipoles that are induced by the applied electric fields as the bias voltage is swept from depletion to accumulation in the capacitance-voltage measurements. Clearly more work is necessary in this area.

This article has not addressed oxidation processes performed at temperatures in excess of 900 °C. For example, it would be interesting to determine whether high temperature thermal or rapid thermal oxidations at temperatures >950 °C induces roughness, i.e., excess suboxide bonding in interfacial transition regions, and to determine the extent to which a 900 °C RTA is effective in reducing any roughness produced.

ACKNOWLEDGMENTS

Support by the Office of Naval Research, the National Science Foundation, and the Semiconductor Research Corporation is greatly appreciated.

- ¹D. Mathiot, A. Straboni, E. Andre, and P. Debenest, *J. Appl. Phys.* **73**, 8215 (1993); J. Ahn, J. Kim, G. Q. Lo, and D.-L. Kwong, *Appl. Phys. Lett.* **60**, 2089 (1992).
- ²D. R. Lee, G. Lucovsky, M. R. Denker, and C. Magee, *J. Vac. Sci. Technol. A* **13**, 607 (1995); D. R. Lee, C. Parker, J. R. Hauser, and G. Lucovsky, *J. Vac. Sci. Technol. B* **13**, 1778 (1995).
- ³G. Lucovsky, H. Niimi, K. Koh, D. R. Lee, and Z. Jing, *The Physics and Chemistry of SiO₂ and the Si–SiO₂ Interface*, edited by H. Z. Massoud, E. H. Poindexter, and C. R. Helms (Electrochemical Society, Pennington, NJ, 1996), p. 441.
- ⁴A. Banerjee and G. Lucovsky, *MRS Symp. Proc.* **420**, 405 (1996).
- ⁵B. Hinds, G. Lucovsky, A. Banerjee, and R. Johnson, *MRS Symp. Proc.* (in press).
- ⁶H.-S. Tao, J. E. Rowe, H. Niimi, H. Yang, T. E. Madey, and G. Lucovsky (unpublished).

- ⁷F. J. Grunthaner and P. J. Grunthaner, *Mater. Sci. Rep.* **1**, 65 (1986).
- ⁸F. J. Himpsel, F. R. McFeely, A. Teleb-Ibrahimi, J. A. Yarnoff, and G. Hollinger, *Phys. Rev. B* **38**, 6084 (1988); M. M. Banaszak-Holl, S. Lee, and F. R. McFeely, *Appl. Phys. Lett.* **65**, 1097 (1994).
- ⁹M.-T. Tang, K. W. Evans-Lutterodt, G. S. Higashi, and T. Boone, *Appl. Phys. Lett.* **62**, 3144 (1993); M. L. Green, D. Brasen, K. W. Evans-Lutterholt, L. C. Feldman, K. Krisch, W. Lennard, H.-T. Tang, L. Manchanda, and M.-T. Tang, *ibid.* **65**, 848 (1994).
- ¹⁰E. P. Gusev, H. C. Lu, T. Gustafsson, and E. Garfunkel, *Phys. Rev. B* **52**, 1759 (1995).
- ¹¹X. Chen and J. M. Gibson, *Appl. Phys. Lett.* **70**, 1462 (1997).
- ¹²T. Yasuda, Y. Ma, S. Habermehl, and G. Lucovsky, *Appl. Phys. Lett.* **60**, 434 (1992).
- ¹³C. H. Bjorkman, T. Yasuda, C. E. Shearon, Jr., U. Emmerichs, C. Meyer, K. Leo, and H. Kurz, *J. Vac. Sci. Technol. B* **11**, 1521 (1993).
- ¹⁴S. S. Chao, J. E. Tyler, Y. Takagi, P. G. Pai, G. Lucovsky, S. Y. Lin, C. K. Wong, and M. J. Mantini, *J. Vac. Sci. Technol. A* **4**, 1574 (1986).
- ¹⁵D. V. Tsu, G. Lucovsky, and B. N. Davidson, *Phys. Rev. B* **40**, 1795 (1989).
- ¹⁶M. A. Paesler, D. A. Anderson, E. C. Freeman, G. Moddel, and W. Paul, *Phys. Rev. Lett.* **41**, 1492 (1978).
- ¹⁷J. C. Knights, R. A. Street, and G. Lucovsky, *J. Non-Cryst. Solids* **35–36**, 279 (1980).
- ¹⁸Y. Kanemitsu, H. Uto, Y. Masumoto, T. Masumoto, T. Futagi, and H. Mimura, *Phys. Rev. B* **48**, 2827 (1993).
- ¹⁹J. Didap, X. F. Hu, M. H. Anderson, M. C. Downer, M. terBeck, J. K. Lowell, and O. A. Aktsipetrov, in *Ref. 2*, p. 406.
- ²⁰T. Sakoda and Matsumura, *Proceedings of ISCSI, Karuizawa, Japan, 1996*.
- ²¹F. M. Ross, J. M. Gibson, and R. D. Twisten, *Surf. Sci.* **310**, 243 (1994).
- ²²P. O. Hahn and M. Henzler, *J. Vac. Sci. Technol. B* **2**, 574 (1984).
- ²³J. R. Hauser (private communication).
- ²⁴J. Stathis (unpublished).